JEM Journal of Experimental Medicine

BRIEF DEFINITIVE REPORT

Neutrophil extracellular traps infiltrate the lung airway, interstitial, and vascular compartments in severe COVID-19

Coraline Radermecker[1,2], Nancy Detrembleur[3,4], Julien Guiot[5,6], Etienne Cavalier[7], Monique Henket[5,6], Céline d'Emal[8], Céline Vanwinge[9], Didier Cataldo[9], Cécile Oury[8]*, Philippe Delvenne[3,4]*, and Thomas Marichal[1,2,10]*

Infection with SARS-CoV-2 is causing a deadly and pandemic disease called coronavirus disease–19 (COVID-19). While SARS-CoV-2–triggered hyperinflammatory tissue-damaging and immunothrombotic responses are thought to be major causes of respiratory failure and death, how they relate to lung immunopathological changes remains unclear. Neutrophil extracellular traps (NETs) can contribute to inflammation-associated lung damage, thrombosis, and fibrosis. However, whether NETs infiltrate particular compartments in severe COVID-19 lungs remains to be clarified. Here we analyzed postmortem lung specimens from four patients who succumbed to COVID-19 and four patients who died from a COVID-19–unrelated cause. We report the presence of NETs in the lungs of each COVID-19 patient. NETs were found in the airway compartment and neutrophil-rich inflammatory areas of the interstitium, while NET-prone primed neutrophils were present in arteriolar microthrombi. Our results support the hypothesis that NETs may represent drivers of severe pulmonary complications of COVID-19 and suggest that NET-targeting approaches could be considered for the treatment of uncontrolled tissue-damaging and thrombotic responses in COVID-19.

Introduction

The COVID-19 pandemic emerged in Wuhan, China, and rapidly spread globally, leading to an overwhelming pressure on health-care systems that required substantial hygienic and containment measures. Severe acute respiratory coronavirus-2 (SARS-CoV-2) has been identified as the etiological agent of COVID-19 (Wu et al., 2020; Bao et al., 2020), whose clinical manifestations range from the absence of symptoms to an acute respiratory distress syndrome (ARDS) and sometimes multi-organ failure, leading to death (Huang et al., 2020; Chen et al., 2020; Guan et al., 2020). While the determinants of disease severity are not completely understood yet, host factors such as age or an excessive inflammatory response to SARS-CoV-2 have been incriminated (Zhang et al., 2020).

The lungs are main targets of COVID-19, and patients with severe forms of the disease are often admitted to the hospital because of ARDS-associated hypoxemia, a consequence of impaired lung ventilation, diffusion, or perfusion (Huang et al., 2020; Chen et al., 2020; Guan et al., 2020). In addition, thrombotic complications have frequently been associated with COVID-19 in critically ill patients, representing a cause of organ failure and death (Zhou et al., 2020; Connors and Levy, 2020; Ackermann et al., 2020; Terpos et al., 2020; Wichmann et al., 2020; Helms et al., 2020). Since no effective therapeutic options exist for COVID-19, a better understanding of the pathophysiological mechanisms involved in the most severe forms of the disease is a pressing medical need (Bikdeli et al., 2020). In this regard, relationships between fatal forms of COVID-19 and lung immunopathological changes remain to be discovered in order to help the clinical management of the disease.

Neutrophils represent the most abundant leukocyte population in the blood. Of note, neutrophilia and elevated serum levels

[1]Laboratory of Immunophysiology, Grappe Interdisciplinaire de Génoprotéomique Appliquée (GIGA) Institute, Liege University, Liege, Belgium; [2]Faculty of Veterinary Medicine, Liege University, Liege, Belgium; [3]Department of Pathology, Clinique Hospitalo-Universitaire (CHU) University Hospital, Liege University, Liege, Belgium; [4]Laboratory of Experimental Pathology, Grappe Interdisciplinaire de Génoprotéomique Appliquée (GIGA) Institute, Liege University, Liege, Belgium; [5]Pneumology department, Clinique Hospitalo-Universitaire (CHU) Liège, Grappe Interdisciplinaire de Génoprotéomique Appliquée (GIGA) Institute, Liege University, Liege, Belgium; [6]Laboratory of Pneumology, Grappe Interdisciplinaire de Génoprotéomique Appliquée (GIGA) Institute, Liege University, Liege, Belgium; [7]Medical Chemistry, Center for Interdisciplinary Research on Medicines Institute, Liege University, Liege, Belgium; [8]Laboratory of Cardiology, Grappe Interdisciplinaire de Génoprotéomique Appliquée (GIGA) Institute, Liege University, Liege, Belgium; [9]Laboratory of Tumor and Development Biology, Grappe Interdisciplinaire de Génoprotéomique Appliquée (GIGA) Institute, Liege University, Liege, Belgium; [10]Walloon Excellence in Life Sciences and Biotechnology, Wallonia, Belgium.

*C. Oury, P. Delvenne, and T. Marichal contributed equally to this paper; Correspondence to Thomas Marichal: t.marichal@uliege.be; Philippe Delvenne: p.delvenne@uliege.be; Cécile Oury: cecile.oury@uliege.be.

of the main neutrophil chemoattractant IL-8 were found in severe cases of COVID-19 and were associated with poor disease outcome (Li et al., 2020; Wang et al., 2020; Zhang et al., 2020). In addition, neutrophils have been shown to infiltrate lungs of hospitalized COVID-19 patients (Barnes et al., 2020; Chen et al., 2020). A powerful feature of activated neutrophils is their ability to form neutrophil extracellular traps (NETs), web-like structures rich in host DNA and containing modified histone proteins and granule proteins such as neutrophil elastase (NE) and myeloperoxidase (MPO; Papayannopoulos, 2018). Initially discovered for their role in bacterial killing (Brinkmann et al., 2004), NETs are now thought to contribute to the pathophysiology of a wide range of infectious or noninfectious diseases (Papayannopoulos, 2018; Jorch and Kubes, 2017). Interestingly, NETs can be formed in the lungs upon infection with respiratory viruses (Schönrich and Raftery, 2016; Radermecker et al., 2019; Toussaint et al., 2017; Narasaraju et al., 2011; Moorthy et al., 2016b; Ashar et al., 2018). Moreover, they have the ability to promote lung damage (Caudrillier et al., 2012; Lefrançais et al., 2018; Narasaraju et al., 2011; Twaddell et al., 2019; Porto and Stein, 2016; Barnes et al., 2020), thrombosis (Ali et al., 2019; Meng et al., 2017; Barnes et al., 2020), and fibrosis (Chrysanthopoulou et al., 2014; Savchenko et al., 2014), three features encountered in severe forms of COVID-19 patients (Ackermann et al., 2020; Wang et al., 2020; Guan et al., 2020; Zhou et al., 2020; Connors and Levy, 2020). Accordingly, NETs have recently been proposed to represent potential drivers of COVID-19, as suggested by several opinion articles (Barnes et al., 2020; Mozzini and Girelli, 2020; Yaqinuddin and Kashir, 2020; Yaqinuddin et al., 2020; Narasaraju et al., 2020; Thierry and Roch, 2020; Tomar et al., 2020). Moreover, NET components have been detected in the sera of COVID-19 patients and correlated with disease severity (Zuo et al., 2020; Middleton et al., 2020).

In the present study, we performed immunofluorescence staining on postmortem lung biopsies from COVID-19 patients to assess whether NET structures could be identified in the lungs of those patients, and whether they were located in particular lesions and micro-anatomical lung compartments. We report the presence of NETs in COVID-19–injured lungs, while they were not detected in lungs from patients who died from another cause. Interestingly, we found that NETs were mainly associated with the inflammatory interstitial lesions and the airways, while NET-prone primed neutrophils were found in pulmonary microcirculation. Our study supports the hypothesis that NETs may contribute to lung pathology in severe COVID-19 and represent putative therapeutic targets.

Results and discussion

Clinical presentation of COVID-19 patients

Postmortem lung samples were collected from four patients who died from COVID-19 at the University Hospital of Liege, Belgium (Table 1). The age ranged from 51 to 73 yr, and one patient was female. Each case tested positive for SARS-CoV-2 by nasopharyngeal swab and RT-PCR at the time of admission. The total duration of the hospitalization until death ranged between 8 and 32 d. Assisted mechanical ventilation was implemented at the time of admission for three patients, and at day 3 after admission for one patient (Table 1). Existing comorbidities and chronic treatments are reported in Table 1. Every patient received in-hospital antiviral (i.e., hydroxychloroquine) and antibiotic therapy. In the last 24 h preceding death, each patient exhibited blood neutrophilia and elevated serum C-reactive protein levels (Table 1). Serum IL-6 levels were elevated in the three patients who were assessed for IL-6, and levels of the fibrin degradation products D-dimers were also above the normal range for the four patients, indicative of ongoing thrombosis and subsequent fibrinolysis (Table 1). Lymphopenia and thrombocytopenia were observed in three out of four patients (Table 1). The identified causes of death were pneumonia, ARDS, or multi-organ failure. Typical lesions of diffuse alveolar damage (Xu et al., 2020) were confirmed by histopathological examination of lung sections by experienced pathologists (Table 1). Hence, the four patients represented prototypical severe and fatal cases of COVID-19, characterized by pneumonia and fatal respiratory distress associated with signs of systemic inflammation, neutrophilia, and coagulopathy (Huang et al., 2020; Chen et al., 2020; Guan et al., 2020; Li et al., 2020; Wang et al., 2020; Tang et al., 2020; Giusti et al., 2020).

NETs are uniquely detected in lung specimens from COVID-19 patients

First, we sought to determine whether NETs could be detected in the lungs of these COVID-19 patients. NETs are released by neutrophils and are defined as extracellular structures containing large amounts of DNA, modified histone proteins such as citrullinated histone H3 (Cit-H3), and granule proteins, including MPO and NE, which both regulate NET formation (Papayannopoulos, 2018; Boeltz et al., 2019). Many methods are being used to detect and quantify NETs (Boeltz et al., 2019). The detection of one single NET component (e.g., cell-free DNA, MPO, NE, Cit-H3) is nonspecific and should therefore be combined with more specific methods. In this regard, assays measuring NE/DNA or MPO/DNA complexes are often used to quantify NET fragments in body fluids or secretions, including the bronchoalveolar lavage fluid (Caudrillier et al., 2012; Bendib et al., 2019; Mikacenic et al., 2018). Nevertheless, immunohistochemistry in tissue section is the most widely used and recommended method, as it allows the unambiguous visualization of extracellular structures containing extracellular DNA and colocalizing with granule-derived proteins and modified histones (Boeltz et al., 2019; Caudrillier et al., 2012; Radermecker et al., 2019; Rocks et al., 2019). We performed immunofluorescence staining on paraffin-embedded lung sections from COVID-19 patients with anti-MPO and anti–Cit-H3 antibodies together with DAPI. Incubation with rabbit and goat sera and secondary antibodies was used as controls (Fig. 1, A–D). We found NETs, defined as extracellular areas triple positive for DNA-bound DAPI, MPO, and Cit-H3 (i.e., $DAPI^+MPO^+Cit\text{-}H3^+$ NETs), in lung sections from COVID-19 patients (Fig. 1, A–H, large arrowheads). We also analyzed lung sections from four "control" patients who died from a COVID-19–unrelated cardiac cause (Table S1). Notably, we were not able to find any $DAPI^+MPO^+Cit\text{-}H3^+$

Table 1. **Demographic and clinical characteristics, and hematological and clinical biochemistry findings of COVID-19 patients**

Patient no.	1	2	3	4
Gender	M	F	M	M
Age (yr)	56	63	51	73
Known comorbidities	Emphysema, extrinsic asthma	Type 2 diabetes, obesity, hyperanxiety, epilepsy	Type 2 diabetes, hypertension, fatty liver	None
Chronic treatments	Inhaled CS and β2 agonists, leukotriene receptor antagonists, SSRI	Anti-diabetes (metformin), neuroleptic (haloperidol), anxiolytic (prothipendyl), anti-epileptic (sodium valproate), L-thyroxin, anti-convulsive (procyclidin)	Anti-diabetes (metformin, empagliflozine), anti-hypertensive (ACE inhibitor, angiotensin 2 receptor antagonist), α1 receptor antagonists	L-thyroxin, aspirin
Time from admission to death (d)	18	8	32	22
Symptom duration before admission (d)	8	7	7	2
Duration of ventilator management (d)	15	8	32	22
Secondary lung infection	No	No	Yes	Yes
Secondary disorder	Renal failure	Pneumothorax	Renal failure, hypercortisolemia	Renal failure, atrial fibrillation
In-hospital antiviral therapy (hydroxychloroquine)	Yes	Yes	Yes	Yes
In-hospital antibiotic therapy	Yes	Yes	Yes	Yes
In-hospital antifungal therapy	No	No	Yes	No
In-hospital anticoagulant therapy (heparin)	Yes	No	No	No
Cause of death	ARDS, multi-organ failure	Pneumonia	ARDS	ARDS
Diffuse alveolar damage	Yes	Yes	Yes	Yes
Lymphocytes [1.1–4.5 10^3/µl]	1.41	0.17[a]	0.97[a]	Below detection[a]
Neutrophils [1.5–4.5 10^3/µl]	25.84[b]	8.7[b]	6.93[b]	18.35[b]
Monocytes [0.1–0.9 10^3/µl]	1.61[b]	0.34	0.75	Below detection[a]
Platelets [150–370 10^3/µl]	7[a]	217	70[a]	26[a]
CRP [0–5 µg/ml]	391.4[b]	286.8[b]	183.3[b]	231[b]
Fibrinogen [1.79–3.86 mg/ml]	4.43[b]	7.55[b]	3.47	5.70[b]
IL-6 [< 1 IU/ml]	Not measured	384.8[b]	129.3[b]	1,077.3[b]
D-dimer [< 500 µg/liter]	2,106[b]	7,440[b]	9,149[b]	4,559[b]

For hematological and clinical biochemistry values, references ranges are indicated in brackets. ACE, angiotensin-converting enzyme; CRP, C-reactive protein; CS, corticosteroids; F, female; M, male; SSRI, selective serotonin reuptake inhibitor.
[a]Values below the reference range.
[b]Values above the reference range.

NETs in lung sections from those non–COVID-19 patients (Fig. 1, A–D; and Fig. S1). Instead, we only sporadically detected MPO^+ neutrophils whose nuclei stained positive for Cit-H3 (Fig. 1, A–D; thin arrow). We quantified the volume of extracellular structures displaying a colocalization between MPO and Cit-H3, i.e., $MPO^+Cit\text{-}H3^+$ NETs, in multiple fields from each patient and confirmed that NETs were uniquely found in COVID-19 lungs, but not in non–COVID-19 control lungs (Fig. 1 I). The absence of NETs in postmortem lung specimens from non–COVID-19 patients rules out the possibility that NETs are formed postmortem, merely as a consequence of death. In addition, in order to address whether the formation of NETs was specific to the lung tissue in COVID-19 patients, we performed similar staining on sections from the liver, pancreas, kidney, and heart from COVID-19 patients for

which such material was available. Of note, we did not find any evidence of NET formation in those organs (Fig. S2), suggesting that the systemic presence of NET components reported in sera from COVID-19 patients (Zuo et al., 2020; Middleton et al., 2020) is not associated with widespread NET formation in peripheral organs.

NETs are distributed in the airway, interstitial, and vascular compartments of COVID-19 lungs

To gain further insights into the relative abundance of NETs in the lungs of COVID-19 patients, we scanned the entire immunofluorescently stained lung sections and marked the zones that were rich in $MPO^+Cit\text{-}H3^+$ NETs. This analysis revealed the presence of multiple, widely distributed NET-infiltrating areas in the lungs of COVID-19 patients (Fig. 2, A and B), as depicted by black circles on consecutive H&E-stained sections (Fig. 2 C).

NETs may contribute to different aspects of COVID-19 physiopathology by infiltrating distinct lung compartments. To determine whether NETs were located in particular microanatomical localizations and lesions, we performed a detailed histopathological analysis of the NET-infiltrating areas for each patient (Table 2).

First, NETs were largely associated with the airway compartment in the four patients (Table 2 and Fig. 3, A and B). Of note, they were often associated with fibrin, and occluded some alveoli or bronchioles almost completely. Extravascular fibrin deposition could result in leakage of plasma proteins, fibrinogen, and thrombi into the airway lumen (Wagers et al., 2004). Therefore, the presence of NETs in the airway compartment may represent major procoagulant triggers, leading to fibrin deposition and subsequent impaired pulmonary ventilation. In advanced stages, NETs could be replaced by collagen networks, thereby contributing to COVID-19–triggered lung fibrosis (Chrysanthopoulou et al., 2014; Savchenko et al., 2014). They may also facilitate secondary infections, such as seen in cystic fibrosis (Porto and Stein, 2016; Barnes et al., 2020). In our study, two out of four patients developed a secondary lung infection during hospitalization (Table 1). Even though NETs may also be induced by bacterial-derived mediators during a secondary infection (Porto and Stein, 2016; Hamaguchi et al., 2012; Moorthy et al., 2016a), we found a massive presence of NETs in each patient, regardless of the status of secondary infection. It is thus unlikely that the secondary infection on its own would be solely responsible for the massive and multifocal infiltration of NETs in our study.

Second, the interstitial compartment also contained NETs in three patients, especially in zones infiltrated by neutrophils and macrophages, while no lymphocytes were observed (Table 2 and Fig. 3 C). The proximity between NET-releasing neutrophils and macrophages is consistent with the hypothesis that NET could contribute to the cytokine storm in COVID-19 (Barnes et al., 2020), by triggering IL-1β secretion from macrophages, which would in turn increase NET formation and IL-6 secretion, as reported in other settings (Kahlenberg et al., 2013; Warnatsch et al., 2015; Meher et al., 2018; Sil et al., 2017).

Third, NET-rich zones encompassed the vascular compartment in lungs from three patients, where they mainly localized in arterioles containing microthrombi (Table 2 and Fig. 3 D). It is important to note that, in microthrombi, we mainly observed numerous $Cit\text{-}H3^+MPO^+$ neutrophils, as reported by others (Middleton et al., 2020), rather than filamentous NETs, supporting that such activated neutrophils are in earlier stages of NET formation. Whether NETs actually contribute to the formation of COVID-19–associated pulmonary microthrombi (Ackermann et al., 2020) merits further investigation. Under conditions of infection-induced lung inflammation, NETs may indeed represent a mechanism by which neutrophils participate in thrombus formation (Laridan et al., 2019; Middleton et al., 2020). NETs form a scaffold for adhesion of platelets (Laridan et al., 2019), adhesion molecules such as von Willebrand factor and fibrinogen, and red blood cells. They mediate histone-induced platelet activation and aggregation. NET components, e.g., histones, DNA, NE, and cathepsin G, also have the ability to activate tissue-factor or factor 12–dependent coagulation, which results in fibrin generation and the formation of platelet- and fibrin-rich thrombi.

General discussion and conclusions

Our study reports that NETs infiltrate distinct compartments and lesions in the lungs of COVID-19 patients with a fatal outcome. It was performed on a small number of patients from the same country and hospital, which is an obvious limitation. In addition, our study does not demonstrate the causality between NETs and COVID-19 pathophysiology, as this would only be revealed in large clinical studies or model systems in which NETs would be targeted. These two points highlight the need for additional studies before drawing definitive conclusions about the implication of NETs in COVID-19 physiopathology.

The assisted mechanical ventilation of the patients represents a potential confounding factor for establishing a direct link between COVID-19 and NETs. Indeed, mechanical ventilation can be injurious to the lungs and has been shown to induce NETs (Yildiz et al., 2015; Porto and Stein, 2016). Yet it is mainly triggering alveolar damage, and would arguably induce NETs in the airway compartment only, but not in the interstitial or vascular compartments. Furthermore, a recent study indicates no relationship between ventilation duration and the amount of NETs in the bronchoalveolar lavage fluid from patients with pneumonia-related ARDS (Bendib et al., 2019). Thus, while we cannot rule out a contribution of the assisted mechanical ventilation to the formation of NETs in COVID-19 patients, it is unlikely that this could explain the widespread distribution of NETs in the lungs of COVID-19 patients.

In-hospital antiviral therapy was administered to each COVID-19 patient (Table 1), which may also influence the production of NETs. Nevertheless, data from the literature indicate that chloroquine exhibits an inhibitory effect on NET formation in other contexts (Boone et al., 2018; Murthy et al., 2019). In addition, we would have expected to see NETs in other organs than the lung if hydroxychloroquine was sufficient to trigger NETs, which was not the case. Further investigations would, however, be necessary to formally exclude an effect of hydroxychloroquine on NETs in COVID-19 lungs.

There is currently no therapy against COVID-19, and several clinical trials are ongoing. Our findings that NETs widely

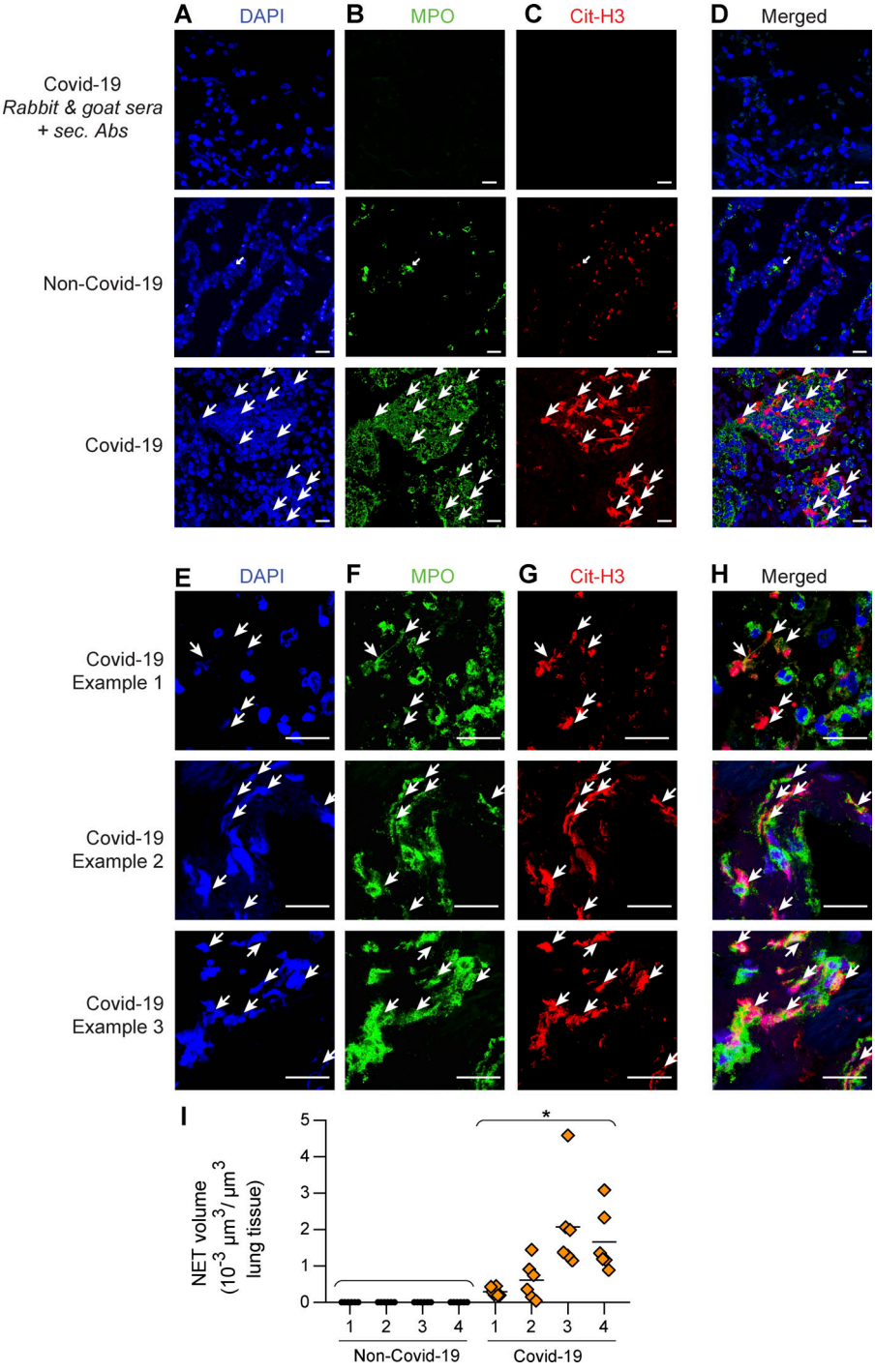

Figure 1. **DAPI⁺MPO⁺Cit-H3⁺ NETs are uniquely detected in lungs of COVID-19 patients. (A–D)** Representative confocal microscopy pictures (magnification, 20×, maximal intensity projections of a Z-stack) of (A) DAPI (blue), (B) MPO (green), (C) Cit-H3 (red), and (D) merged stainings from non–COVID-19 and COVID-19 lungs. Control sections were incubated with rabbit and goat sera and with secondary antibodies (sec. Abs). Pictures are representative of one of four non–COVID-19 and one of four COVID-19 patients analyzed. Extracellular DAPI⁺MPO⁺Cit-H3⁺ NETs are indicated by large arrowheads, while one MPO⁺Cit-H3⁺ neutrophil is indicated by a thin arrow. **(E–H)** Representative high-resolution confocal microscopy pictures (magnification, 63×, maximal intensity projections of a Z-stack) of (E) DAPI (blue), (F) MPO (green), (G) Cit-H3 (red), and (H) merged stainings from COVID-19 lungs. DAPI⁺MPO⁺Cit-H3⁺ NETs are indicated by large arrowheads. **(I)** Quantification of NET volume from multiple fields (20×) of lung sections from the four non–COVID-19 and the four COVID-19 patients. Results show individual values and mean. P value compares non–COVID-19 and COVID-19 samples and was calculated using a nonparametric Mann–Whitney *U* test on mean values. *, $P < 0.05$. Scale bars, 20 µm.

infiltrate the lungs of deceased patients can be of major importance. On the one hand, thrombotic events have been suspected to contribute to COVID-19 morbidity and mortality, and current interim guidelines recommend the use of heparin regimens for thromboprophylaxis and anticoagulation treatment (Spyropoulos et al., 2020; Bikdeli et al., 2020). Targeting NETs may represent another potential antithrombotic approach that might prove to be beneficial against both immunothrombosis and venous thromboembolism (Barnes et al., 2020; Middleton et al., 2020). In a clinical study of patients with acute coronary syndrome, DNase, an enzyme that breaks down NETs, has been shown to accelerate lysis of coronary thrombi (Mangold et al., 2015). It is also interesting to note that the prothrombotic effect of NETs could be diminished by heparin (Grässle et al., 2014), providing further support of current recommendations. On the other hand, dysregulated NET formation could aggravate lung damage and the impairment of gas exchanges (Caudrillier et al., 2012; Lefrançais et al., 2018; Narasaraju et al., 2011; Twaddell et al., 2019; Porto and Stein, 2016; Barnes et al., 2020). Inhalation of human recombinant DNase I (pulmozyme/dornase α) has been shown to improve lung function and to reduce secondary infections in cystic fibrosis

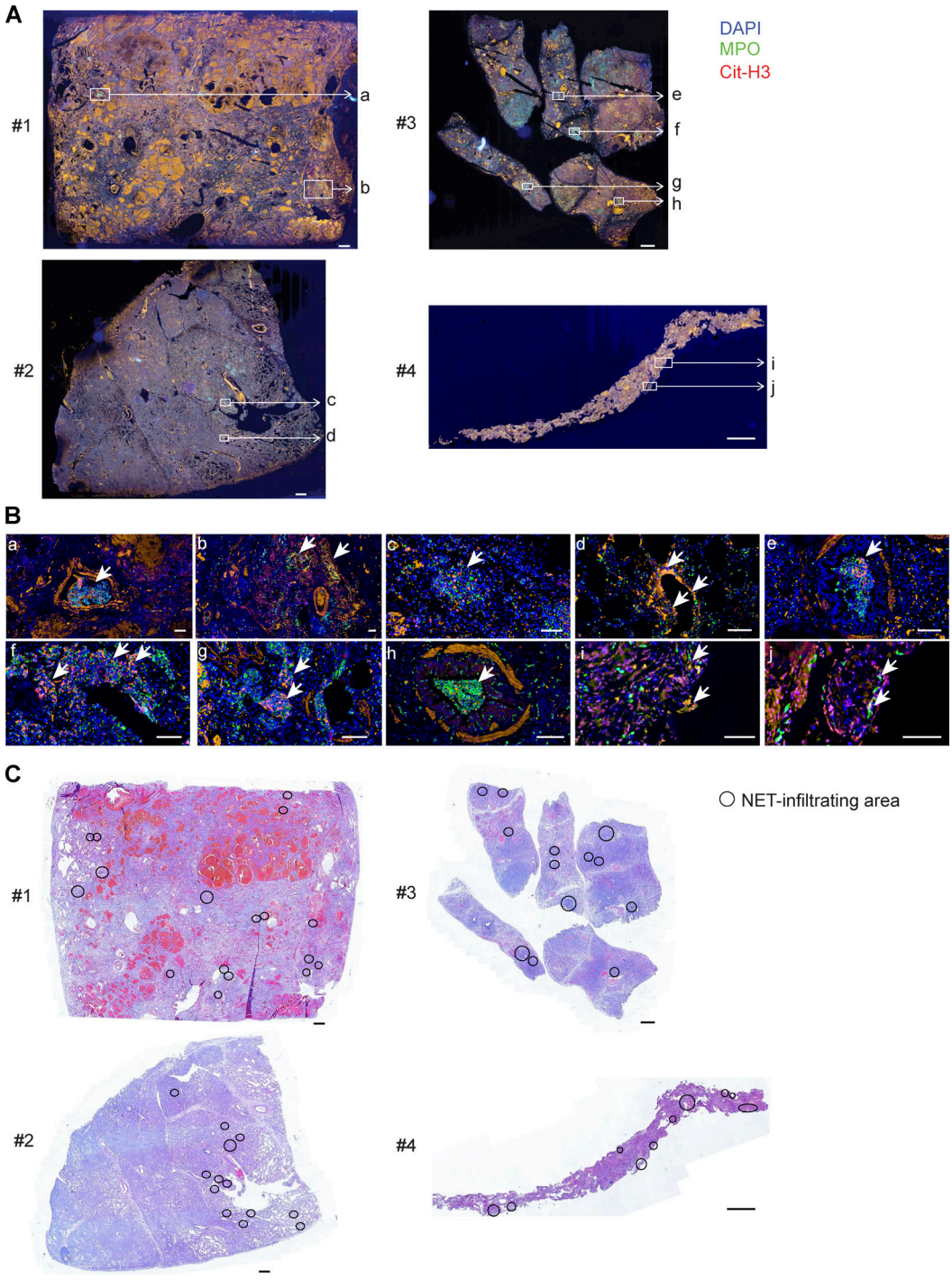

Figure 2. **NETs are broadly distributed in postmortem lung specimens from COVID-19 patients. (A)** Photographs of entire antibody-stained immunofluorescence lung sections from COVID-19 patients. **(B)** Magnification of NET-rich zones, indicated by white boxes in A. $MPO^+Cit\text{-}H3^+$ NETs are indicated by large arrowheads. **(C)** Photographs of entire H&E-stained lung sections from COVID-19 patients. NET-infiltrating areas are circled in black. Scale bars, 1 mm (A and C); 100 µm (B).

(Fuchs et al., 1994; Konstan et al., 2011), and may be beneficial in the context of COVID-19. In this regard, the Efficacy and Safety of Aerosolized Intra-tracheal Dornase Alfa Administration in Patients with COVID-19–Induced ARDS (COVI-Dornase) clinical trial is currently investigating the potential benefit of aerosolized dornase α administration in hospitalized COVID-19 patients suffering from ARDS (Desilles et al., 2020). Altogether, our study supports the idea that targeting NETs in COVID-19 patients may help the clinical management of severe forms of COVID-19 by alleviating thrombotic events, excessive tissue-damaging inflammation, fibrosis, and airway obstruction.

Table 2. **Lung histopathological analysis of NET-infiltrating area in COVID-19 patients**

Patient no.		1	2	3	4
No. of NET-infiltrating area identified	Total	17	13	14	10
	Vascular compartment	6	1	1	0
	Interstitial compartment	2	0	2	7
	Alveolar compartment	9	13	5	5
	Bronchial compartment	0	0	8	0
Alveolar lesions	Inflammation	PMN, macrophages, fibrin, giant and atypical cells	PMN, macrophages, fibrin, giant and atypical cells	PMN, macrophages, fibrin, rare atypical cells	PMN, macrophages, fibrin, hyaline membranes
	Hemorrhage	+	–	+	–
Bronchial lesions	Inflammation	/	/	Intra- and peri-bronchial: PMN, macrophages; rare red blood cells and desquamative epithelial cells	/
Interstitial lesions	Inflammation	PMN, macrophages, fibrin, giant cell, atypical cells	/	PMN, macrophages, fibrin	PMN, fibrin
	Hemorrhage	+	/	+	–
	Fibrosis	+	/	+	+
Vascular lesions	Thrombi	+	+	+	/
	Affected vessels	Arterioles	Arterioles	Arterioles	/
	Other	PMN, fibrin, red blood cells	Fibrin	Fibrin, PMN	/

Some NET-infiltrating areas encompassed several compartments. /, not applicable (no NET detected in the indicated compartment); –, absent; +, present; PMN, polymorphonuclear leukocytes.

Materials and methods

Ethics approval

The use of human specimens was approved in 2020 by the Ethics Reviewing Board of the University Hospital of Liege, Belgium (ref. 2020/119).

Human biopsies

We analyzed lung postmortem biopsy specimens from four patients who died from SARS-CoV-2 infection at the University Hospital of Liege (Belgium) and from four patients who died at the same hospital from a COVID-19–unrelated cause. The non–COVID-19 lung controls were archived tissues that were chosen for the best possible match with respect to age and sex. The characteristics of the patients are presented in Table 1 and Table S1. We also analyzed postmortem biopsy specimens isolated from the liver, heart, kidney, and pancreas from two COVID-19 patients for which such material was available. All tissues were provided by the Biobank of the Liege University Hospital and selected by two pathologists after H&E staining.

Hematology and biochemistry of COVID-19 patients

Hematology and blood biochemistry of COVID-19 patients were retrospectively analyzed. We used the last available blood sample taken in the 24 h preceding the patient's death. All biomarkers have been analyzed by the central laboratory (Hematology and Biochemistry) of the Liege University Hospital.

Histopathological characterization of lungs from COVID-19 patients

The samples were formalin-fixed paraffin-embedded (FFPE), and serial tissue sections of 4 µm were cut for histological and immunofluorescence examination. H&E-stained whole slides were digitized by using a Pannoramic 250 Flash III Scanner (3DHISTECH Ltd.). High-resolution images focused on immunofluorescence-detected NET areas were then assessed by two experienced pathologists by using a scoring system of lesions typically found in SARS-CoV-2 diffuse alveolar damage (Xu et al., 2020) and present in the different lung tissue compartments (alveolar, bronchial, interstitial, and vascular; Table 2).

Immunofluorescence staining and analysis

To identify NETs from lung tissues, lung tissues were FFPE, and lung sections were cut (4-µm-thick sections) for immunofluorescence staining. After deparaffinization and rehydration, tissue sections were boiled for 20 min in 10-mM sodium carbonate buffer for antigen retrieval. Lung sections were permeabilized in PBS 0.5% Triton X-100.

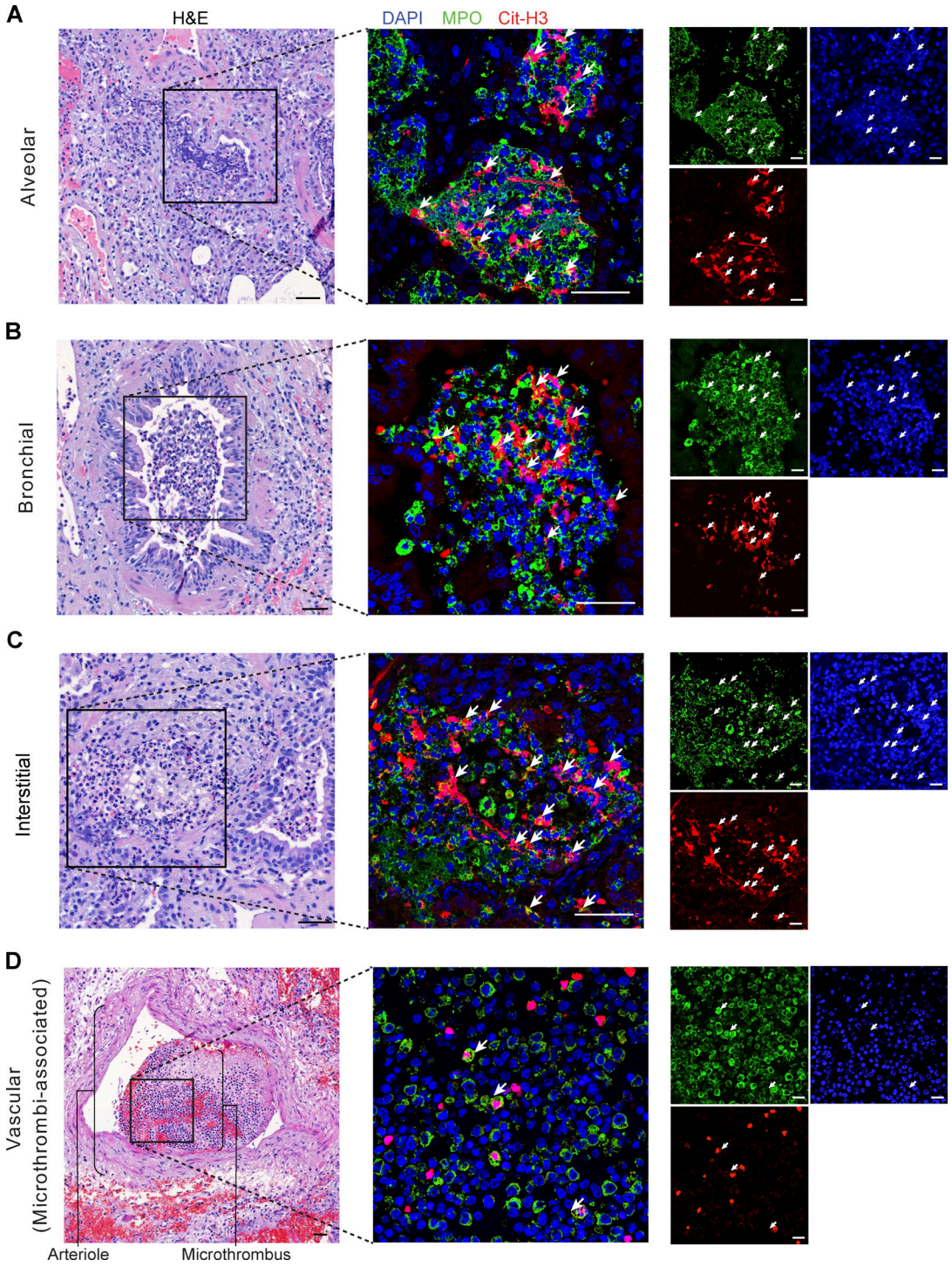

Figure 3. **NETs are found in lesional areas of the lung airway, interstitial, and vascular compartments. (A–D)** Representative pictures of H&E staining from lung sections are shown on the left, and representative pictures of immunofluorescence staining from adjacent lung sections are shown on the right (MPO [red] and Cit-H3 [red] merged with DAPI [blue]). The black box on the left indicates the zone shown by immunofluorescence on the right. $MPO^+Cit\text{-}H3^+$ NETs are indicated by arrowheads. Examples of NETs found (A) in a terminal bronchiole and alveoli, (B) in small bronchi, (C) in the interstitial compartment, and (D) in a microthrombus within an arteriole are shown. Scale bars, 50 µm.

Samples were incubated with a blocking buffer (PBS with 2% BSA and 2% of donkey serum; Sigma-Aldrich) for 1 h at room temperature and stained in blocking buffer with rabbit anti-human antibodies directed against citrullinated histone H3 (Abcam, Ab5103; 1:100 in blocking buffer) and with goat anti-human antibodies directed against MPO (R&D Systems, AF3667; 1:40 in blocking buffer) for 1 h at room temperature. After washing samples with PBS, secondary donkey anti-rabbit IgG antibodies conjugated with Alexa Fluor 568 (1:200 in blocking buffer) and donkey anti-goat IgG antibodies conjugated with Alexa

Fluor 488 (1:200 in blocking buffer) were added in blocking buffer containing DAPI (1:1,000) and incubated for 2 h in the dark at room temperature. Finally, samples were mounted with 10 µl of ProLong Antifade reagent (Thermo Fisher Scientific) on glass slides and stored at room temperature in the dark overnight.

All samples were analyzed by fluorescence microscopy using standard filter sets. Controls were stained with secondary antibodies after incubation with sera from host species (i.e., rabbit and goat sera, 2% in PBS) without primary antibodies, and nonspecific fluorescent staining was not detected under these conditions (Fig. 1, A–D). Images were acquired on a Zeiss LSM 880 Airyscan Elyra S.1. confocal microscope (Zeiss) and processed using ImageJ software.

To quantify the volume of NETs present in the lung tissue, six fields (magnification, 20×) were analyzed per patients, Z-stack pictures were acquired, and Imaris software was used, as described previously (Radermecker et al., 2019). Briefly, we performed a three-dimensional reconstruction of structures staining double positive for Cit-H3 (red) and MPO (green), and Imaris provided quantification of the volume of these structures, expressed as cubic micrometer per cubic micrometer of lung tissue. The colocalization analysis method uses three Imaris script/macro tools. The first script processes all the .ims files in a folder. The script thresholds the red Cit-H3 and the green MPO staining. Then, we created a new channel, i.e., the intersection between red threshold and green threshold, where all the voxels have a colocalization equal to 1. Then, the second script measured the volume of the intersection between the red threshold and the green threshold. Finally, the third script measured the total volume of the picture. The script created an Excel .xlsx file containing all the measurements.

To assess for the presence of NETs in entire lung sections, sections were entirely scanned using the Nanozoomer 2.0-HT system equipped with a TRI-CCD camera (0.46 µm/pixel [20×] scanning resolution). Sections were manually screened for the presence of areas rich in structures staining double positive for Cit-H3 and MPO, which were identified as NET-infiltrating areas as marked in Fig. 2 C.

Statistical analyses

Data in Fig. 1 I are presented as mean and individual values and were analyzed for statistical significance using a nonparametric Mann–Whitney *U* test on mean values, as indicated in the figure legend. P values <0.05 are considered statistically significant.

Online supplemental material

Fig. S1 shows microscopy pictures of immunofluorescence lung sections from non–COVID-19 patients stained with DAPI, anti-MPO, and anti–Cit-H3 antibodies. Fig. S2 shows representative confocal microscopy pictures of immunofluorescence staining from liver, pancreas, kidney, and heart sections from COVID-19 patients stained with DAPI, anti-MPO, and anti–Cit-H3 antibodies. Table S1 contains demographic and clinical characteristics of the non–COVID-19 patients involved in the study.

Acknowledgments

We thank Dr Alexandre Hego from the Grappe Interdisciplinaire de Génoprotéomique Appliquée Flow Cytometry and Cell Imaging Platform; Dr Benoît Misset, Head of the Intensive Care Unit Department; Dr. Alexandra Belayew for helpful discussions; and Pauline Maréchal, Raja Fares, and Ilham Sbai for their excellent technical and administrative support.

C. Oury is Research Director at the National Funds for Scientific Research, Belgium. P. Delvenne is supported by the Leon Fredericq Foundation (Liege, Belgium). T. Marichal is supported by an "Incentive Grant for Scientific Research" of the National Funds for Scientific Research, Belgium (grant no. F.4508.18), by the FRFS-WELBIO (Walloon Excellence in Life Sciences and Biotechnology; grant no. CR-2019s-04R), by the Acteria Foundation, and by an European Research Council Starting Grant (grant no. ERC-StG-2018 IM-ID 801823).

Author contributions: C. Radermecker, C. Oury, P. Delvenne, and T. Marichal conceived the project and were involved in experimental design. C. Radermecker performed most experiments, and analyzed and compiled the data. C. Radermecker and T. Marichal prepared the figures. N. Detrembleur and P. Delvenne performed histopathological analyses of COVID-19 lungs. J. Guiot collected lung samples from COVID-19 patients. E. Cavalier performed clinical biochemistry measurements. M. Henket was involved in the quantification and compilation of hematological parameters. C. d'Emal collected patients' demographic and clinical characteristics with the help of C. Oury. C. Vanwing and D. Cataldo performed scanning of entire immunofluorescence sections. P. Delvenne selected relevant FFPE material. C. Oury, P. Delvenne, and T. Marichal supervised the study and wrote the manuscript. All authors provided feedback on the manuscript.

Disclosures: E. Cavalier reported "other" from Diasorin, Fujirebio, BioMerieux, IDS, Menarini, and Nittobo outside the submitted work. No other disclosures were reported.

Submitted: 2 June 2020
Revised: 10 July 2020
Accepted: 10 August 2020

References

Ackermann, M., S.E. Verleden, M. Kuehnel, A. Haverich, T. Welte, F. Laenger, A. Vanstapel, C. Werlein, H. Stark, A. Tzankov, et al. 2020. Pulmonary Vascular Endothelialitis, Thrombosis, and Angiogenesis in Covid-19. *N. Engl. J. Med.* 383:120–128. https://doi.org/10.1056/NEJMoa2015432

Ali, R.A., A.A. Gandhi, H. Meng, S. Yalavarthi, A.P. Vreede, S.K. Estes, O.R. Palmer, P.L. Bockenstedt, D.J. Pinsky, J.M. Greve, et al. 2019. Adenosine receptor agonism protects against NETosis and thrombosis in antiphospholipid syndrome. *Nat. Commun.* 10:1916. https://doi.org/10.1038/s41467-019-09801-x

Ashar, H.K., N.C. Mueller, J.M. Rudd, T.A. Snider, M. Achanta, M. Prasanthi, S. Pulavendran, P.G. Thomas, A. Ramachandran, J.R. Malayer, et al. 2018. The Role of Extracellular Histones in Influenza Virus Pathogenesis. *Am. J. Pathol.* 188:135–148. https://doi.org/10.1016/j.ajpath.2017.09.014

Bao, L., W. Deng, B. Huang, H. Gao, J. Liu, L. Ren, Q. Wei, P. Yu, Y. Xu, F. Qi, et al. 2020. The pathogenicity of SARS-CoV-2 in hACE2 transgenic mice. *Nature.* 583:830–833. https://doi.org/10.1038/s41586-020-2312-y

Barnes, B.J., J.M. Adrover, A. Baxter-Stoltzfus, A. Borczuk, J. Cools-Lartigue, J.M. Crawford, J. Daßler-Plenker, P. Guerci, C. Huynh, J.S. Knight, et al. 2020. Targeting potential drivers of COVID-19: Neutrophil extracellular traps. *J. Exp. Med.* 217. e20200652. https://doi.org/10.1084/jem.20200652

Bendib, I., L. de Chaisemartin, V. Granger, F. Schlemmer, B. Maitre, S. Hüe, M. Surenaud, A. Beldi-Ferchiou, G. Carteaux, K. Razazi, et al. 2019. Neutrophil Extracellular Traps Are Elevated in Patients with Pneumonia-

related Acute Respiratory Distress Syndrome. *Anesthesiology*. 130:581–591. https://doi.org/10.1097/ALN.0000000000002619

Bikdeli, B., M.V. Madhavan, A. Gupta, D. Jimenez, J.R. Burton, C. Der Nigoghossian, T. Chuich, S.N. Nouri, I. Dreyfus, E. Driggin, et al; Global COVID-19 Thrombosis Collaborative Group. 2020. Pharmacological Agents Targeting Thromboinflammation in COVID-19: Review and Implications for Future Research. *Thromb. Haemost*. 120:1004–1024. https://doi.org/10.1055/s-0040-1713152

Boeltz, S., P. Amini, H.-J. Anders, F. Andrade, R. Bilyy, S. Chatfield, I. Cichon, D.M. Clancy, J. Desai, T. Dumych, et al. 2019. To NET or not to NET: current opinions and state of the science regarding the formation of neutrophil extracellular traps. *Cell Death Differ*. 26:395–408. https://doi.org/10.1038/s41418-018-0261-x

Boone, B.A., P. Murthy, J. Miller-Ocuin, W.R. Doerfler, J.T. Ellis, X. Liang, M.A. Ross, C.T. Wallace, J.L. Sperry, M.T. Lotze, et al. 2018. Chloroquine reduces hypercoagulability in pancreatic cancer through inhibition of neutrophil extracellular traps. *BMC Cancer*. 18:678. https://doi.org/10.1186/s12885-018-4584-2

Brinkmann, V., U. Reichard, C. Goosmann, B. Fauler, Y. Uhlemann, D.S. Weiss, Y. Weinrauch, and A. Zychlinsky. 2004. Neutrophil extracellular traps kill bacteria. *Science*. 303:1532–1535. https://doi.org/10.1126/science.1092385

Caudrillier, A., K. Kessenbrock, B.M. Gilliss, J.X. Nguyen, M.B. Marques, M. Monestier, P. Toy, Z. Werb, and M.R. Looney. 2012. Platelets induce neutrophil extracellular traps in transfusion-related acute lung injury. *J. Clin. Invest*. 122:2661–2671. https://doi.org/10.1172/JCI61303

Chen, N., M. Zhou, X. Dong, J. Qu, F. Gong, Y. Han, Y. Qiu, J. Wang, Y. Liu, Y. Wei, et al. 2020. Epidemiological and clinical characteristics of 99 cases of 2019 novel coronavirus pneumonia in Wuhan, China: a descriptive study. *Lancet*. 395:507–513. https://doi.org/10.1016/S0140-6736(20)30211-7

Chrysanthopoulou, A., I. Mitroulis, E. Apostolidou, S. Arelaki, D. Mikroulis, T. Konstantinidis, E. Sivridis, M. Koffa, A. Giatromanolaki, D.T. Boumpas, et al. 2014. Neutrophil extracellular traps promote differentiation and function of fibroblasts. *J. Pathol*. 233:294–307. https://doi.org/10.1002/path.4359

Connors, J.M., and J.H. Levy. 2020. COVID-19 and its implications for thrombosis and anticoagulation. *Blood*. 135:2033–2040. https://doi.org/10.1182/blood.2020006000

Desilles, J.P., C. Gregoire, C. Le Cossec, J. Lambert, O. Mophawe, M.R. Losser, F. Lambiotte, S. Le Tacon, M. Cantier, N. Engrand, et al. 2020. Efficacy and safety of aerosolized intra-tracheal dornase alfa administration in patients with SARS-CoV-2-induced acute respiratory distress syndrome (ARDS): a structured summary of a study protocol for a randomised controlled trial. *Trials*. 21:548. https://doi.org/10.1186/s13063-020-04488-8

Fuchs, H.J., D.S. Borowitz, D.H. Christiansen, E.M. Morris, M.L. Nash, B.W. Ramsey, B.J. Rosenstein, A.L. Smith, and M.E. Wohl; The Pulmozyme Study Group. 1994. Effect of aerosolized recombinant human DNase on exacerbations of respiratory symptoms and on pulmonary function in patients with cystic fibrosis. *N. Engl. J. Med*. 331:637–642. https://doi.org/10.1056/NEJM199409083311003

Giusti, B., A.M. Gori, M. Alessi, A. Rogolino, E. Lotti, D. Poli, E. Sticchi, A. Bartoloni, A. Morettini, C. Nozzoli, et al. 2020. Sars-CoV-2 Induced Coagulopathy and Prognosis in Hospitalized Patients: A Snapshot from Italy. *Thromb. Haemost*. 120:1233–1236. https://doi.org/10.1055/s-0040-1712918

Grässle, S., V. Huck, K.I. Pappelbaum, C. Gorzelanny, C. Aponte-Santamaría, C. Baldauf, F. Gräter, R. Schneppenheim, T. Obser, and S.W. Schneider. 2014. von Willebrand factor directly interacts with DNA from neutrophil extracellular traps. *Arterioscler. Thromb. Vasc. Biol*. 34:1382–1389. https://doi.org/10.1161/ATVBAHA.113.303016

Guan, W.-J., Z.-Y. Ni, Y. Hu, W.-H. Liang, C.-Q. Ou, J.-X. He, L. Liu, H. Shan, C.-L. Lei, D.S.C. Hui, et al; China Medical Treatment Expert Group for Covid-19. 2020. Clinical Characteristics of Coronavirus Disease 2019 in China. *N. Engl. J. Med*. 382:1708–1720. https://doi.org/10.1056/NEJMoa2002032

Hamaguchi, S., M. Seki, N. Yamamoto, T. Hirose, N. Matsumoto, T. Irisawa, R. Takegawa, T. Shimazu, and K. Tomono. 2012. Case of invasive nontypable Haemophilus influenzae respiratory tract infection with a large quantity of neutrophil extracellular traps in sputum. *J. Inflamm. Res*. 5:137–140. https://doi.org/10.2147/JIR.S39497

Helms, J., C. Tacquard, F. Severac, I. Leonard-Lorant, M. Ohana, X. Delabranche, H. Merdji, R. Clere-Jehl, M. Schenck, F. Fagot Gandet, et al; CRICS TRIGGERSEP Group (Clinical Research in Intensive Care and Sepsis Trial Group for Global Evaluation and Research in Sepsis). 2020. High risk of thrombosis in patients with severe SARS-CoV-2 infection: a multicenter prospective cohort study. *Intensive Care Med*. 46:1089–1098. https://doi.org/10.1007/s00134-020-06062-x

Huang, C., Y. Wang, X. Li, L. Ren, J. Zhao, Y. Hu, L. Zhang, G. Fan, J. Xu, X. Gu, et al. 2020. Clinical features of patients infected with 2019 novel coronavirus in Wuhan, China. *Lancet*. 395:497–506. https://doi.org/10.1016/S0140-6736(20)30183-5

Jorch, S.K., and P. Kubes. 2017. An emerging role for neutrophil extracellular traps in noninfectious disease. *Nat. Med*. 23:279–287. https://doi.org/10.1038/nm.4294

Kahlenberg, J.M., C. Carmona-Rivera, C.K. Smith, and M.J. Kaplan. 2013. Neutrophil extracellular trap-associated protein activation of the NLRP3 inflammasome is enhanced in lupus macrophages. *J. Immunol*. 190:1217–1226. https://doi.org/10.4049/jimmunol.1202388

Konstan, M.W., J.S. Wagener, D.J. Pasta, S.J. Millar, J.R. Jacobs, A. Yegin, and W.J. Morgan; Scientific Advisory Group and Investigators and Coordinators of Epidemiologic Study of Cystic Fibrosis. 2011. Clinical use of dornase alpha is associated with a slower rate of FEV1 decline in cystic fibrosis. *Pediatr. Pulmonol*. 46:545–553. https://doi.org/10.1002/ppul.21388

Laridan, E., K. Martinod, and S.F. De Meyer. 2019. Neutrophil Extracellular Traps in Arterial and Venous Thrombosis. *Semin. Thromb. Hemost*. 45:86–93. https://doi.org/10.1055/s-0038-1677040

Lefrançais, E., B. Mallavia, H. Zhuo, C.S. Calfee, and M.R. Looney. 2018. Maladaptive role of neutrophil extracellular traps in pathogen-induced lung injury. *JCI Insight*. 3. e98178. https://doi.org/10.1172/jci.insight.98178

Li, S., L. Jiang, X. Li, F. Lin, Y. Wang, B. Li, T. Jiang, W. An, S. Liu, H. Liu, et al. 2020. Clinical and pathological investigation of patients with severe COVID-19. *JCI Insight*. 5. e138070. https://doi.org/10.1172/jci.insight.138070

Mangold, A., S. Alias, T. Scherz, T. Hofbauer, J. Jakowitsch, A. Panzenböck, D. Simon, D. Laimer, C. Bangert, A. Kammerlander, et al. 2015. Coronary neutrophil extracellular trap burden and deoxyribonuclease activity in ST-elevation acute coronary syndrome are predictors of ST-segment resolution and infarct size. *Circ. Res*. 116:1182–1192. https://doi.org/10.1161/CIRCRESAHA.116.304944

Meher, A.K., M. Spinosa, J.P. Davis, N. Pope, V.E. Laubach, G. Su, V. Serbulea, N. Leitinger, G. Ailawadi, and G.R. Upchurch, Jr.. 2018. Novel Role of IL (Interleukin)-1β in Neutrophil Extracellular Trap Formation and Abdominal Aortic Aneurysms. *Arterioscler. Thromb. Vasc. Biol*. 38:843–853. https://doi.org/10.1161/ATVBAHA.117.309897

Meng, H., S. Yalavarthi, Y. Kanthi, L.F. Mazza, M.A. Elfline, C.E. Luke, D.J. Pinsky, P.K. Henke, and J.S. Knight. 2017. In Vivo Role of Neutrophil Extracellular Traps in Antiphospholipid Antibody-Mediated Venous Thrombosis. *Arthritis Rheumatol*. 69:655–667. https://doi.org/10.1002/art.39938

Middleton, E.A., X.-Y. He, F. Denorme, R.A. Campbell, D. Ng, S.P. Salvatore, M. Mostyka, A. Baxter-Stoltzfus, A.C. Borczuk, M. Loda, et al. 2020. Neutrophil Extracellular Traps (NETs) Contribute to Immunothrombosis in COVID-19 Acute Respiratory Distress Syndrome. *Blood*. blood.2020007008. https://doi.org/10.1182/blood.2020007008

Mikacenic, C., R. Moore, V. Dmyterko, T.E. West, W.A. Altemeier, W.C. Liles, and C. Lood. 2018. Neutrophil extracellular traps (NETs) are increased in the alveolar spaces of patients with ventilator-associated pneumonia. *Crit. Care*. 22:358. https://doi.org/10.1186/s13054-018-2290-8

Moorthy, A.N., P. Rai, H. Jiao, S. Wang, K.B. Tan, L. Qin, H. Watanabe, Y. Zhang, N. Teluguakula, and V.T.K. Chow. 2016a. Capsules of virulent pneumococcal serotypes enhance formation of neutrophil extracellular traps during in vivo pathogenesis of pneumonia. *Oncotarget*. 7:19327–19340. https://doi.org/10.18632/oncotarget.8451

Moorthy, A.N., K.B. Tan, S. Wang, T. Narasaraju, and V.T. Chow. 2016b. Effect of High-Fat Diet on the Formation of Pulmonary Neutrophil Extracellular Traps during Influenza Pneumonia in BALB/c Mice. *Front. Immunol*. 7:289. https://doi.org/10.3389/fimmu.2016.00289

Mozzini, C., and D. Girelli. 2020. The role of Neutrophil Extracellular Traps in Covid-19: Only an hypothesis or a potential new field of research? *Thromb. Res*. 191:26–27. https://doi.org/10.1016/j.thromres.2020.04.031

Murthy, P., A.D. Singhi, M.A. Ross, P. Loughran, P. Paragomi, G.I. Papachristou, D.C. Whitcomb, A.H. Zureikat, M.T. Lotze, H.J. Zeh Iii, et al. 2019. Enhanced Neutrophil Extracellular Trap Formation in Acute Pancreatitis Contributes to Disease Severity and Is Reduced by Chloroquine. *Front. Immunol*. 10:28. https://doi.org/10.3389/fimmu.2019.00028

Narasaraju, T., E. Yang, R.P. Samy, H.H. Ng, W.P. Poh, A.-A. Liew, M.C. Phoon, N. van Rooijen, and V.T. Chow. 2011. Excessive neutrophils and neutrophil extracellular traps contribute to acute lung injury of influenza pneumonitis. *Am. J. Pathol.* 179:199–210. https://doi.org/10.1016/j.ajpath.2011.03.013

Narasaraju, T., B.M. Tang, M. Herrmann, S. Muller, V.T.K. Chow, and M. Radic. 2020. Neutrophilia and NETopathy as Key Pathologic Drivers of Progressive Lung Impairment in Patients With COVID-19. *Front. Pharmacol.* 11:870. https://doi.org/10.3389/fphar.2020.00870

Papayannopoulos, V. 2018. Neutrophil extracellular traps in immunity and disease. *Nat. Rev. Immunol.* 18:134–147. https://doi.org/10.1038/nri.2017.105

Porto, B.N., and R.T. Stein. 2016. Neutrophil Extracellular Traps in Pulmonary Diseases: Too Much of a Good Thing? *Front. Immunol.* 7:311. https://doi.org/10.3389/fimmu.2016.00311

Radermecker, C., C. Sabatel, C. Vanwinge, C. Ruscitti, P. Maréchal, F. Perin, J. Schyns, N. Rocks, M. Toussaint, D. Cataldo, et al. 2019. Locally instructed CXCR4^{hi} neutrophils trigger environment-driven allergic asthma through the release of neutrophil extracellular traps. *Nat. Immunol.* 20:1444–1455. https://doi.org/10.1038/s41590-019-0496-9

Rocks, N., C. Vanwinge, C. Radermecker, S. Blacher, C. Gilles, R. Marée, A. Gillard, B. Evrard, C. Pequeux, T. Marichal, et al. 2019. Ozone-primed neutrophils promote early steps of tumour cell metastasis to lungs by enhancing their NET production. *Thorax.* 74:768–779. https://doi.org/10.1136/thoraxjnl-2018-211990

Savchenko, A.S., K. Martinod, M.A. Seidman, S.L. Wong, J.I. Borissoff, G. Piazza, P. Libby, S.Z. Goldhaber, R.N. Mitchell, and D.D. Wagner. 2014. Neutrophil extracellular traps form predominantly during the organizing stage of human venous thromboembolism development. *J. Thromb. Haemost.* 12:860–870. https://doi.org/10.1111/jth.12571

Schönrich, G., and M.J. Raftery. 2016. Neutrophil Extracellular Traps Go Viral. *Front. Immunol.* 7:366. https://doi.org/10.3389/fimmu.2016.00366

Sil, P., H. Wicklum, C. Surell, and B. Rada. 2017. Macrophage-derived IL-1β enhances monosodium urate crystal-triggered NET formation. *Inflamm. Res.* 66:227–237. https://doi.org/10.1007/s00011-016-1008-0

Spyropoulos, A.C., J.H. Levy, W. Ageno, J.M. Connors, B.J. Hunt, T. Iba, M. Levi, C.M. Samama, J. Thachil, D. Giannis, et al; Subcommittee on Perioperative, Critical Care Thrombosis, Haemostasis of the Scientific, Standardization Committee of the International Society on Thrombosis and Haemostasis. 2020. Scientific and Standardization Committee communication: Clinical guidance on the diagnosis, prevention, and treatment of venous thromboembolism in hospitalized patients with COVID-19. *J. Thromb. Haemost.* 18:1859–1865. https://doi.org/10.1111/jth.14929

Tang, N., D. Li, X. Wang, and Z. Sun. 2020. Abnormal coagulation parameters are associated with poor prognosis in patients with novel coronavirus pneumonia. *J. Thromb. Haemost.* 18:844–847. https://doi.org/10.1111/jth.14768

Terpos, E., I. Ntanasis-Stathopoulos, I. Elalamy, E. Kastritis, T.N. Sergentanis, M. Politou, T. Psaltopoulou, G. Gerotziafas, and M.A. Dimopoulos. 2020. Hematological findings and complications of COVID-19. *Am. J. Hematol.* 95:834–847. https://doi.org/10.1002/ajh.25829

Thierry, A.R., and B. Roch. 2020. SARS-CoV2 may evade innate immune response, causing uncontrolled neutrophil extracellular traps formation and multi-organ failure. *Clin. Sci. (Lond.).* 134:1295–1300. https://doi.org/10.1042/CS20200531

Tomar, B., H.-J. Anders, J. Desai, and S.R. Mulay. 2020. Neutrophils and Neutrophil Extracellular Traps Drive Necroinflammation in COVID-19. *Cells.* 9:1383. https://doi.org/10.3390/cells9061383

Toussaint, M., D.J. Jackson, D. Swieboda, A. Guedán, T.D. Tsourouktsoglou, Y.M. Ching, C. Radermecker, H. Makrinioti, J. Aniscenko, N.W. Bartlett, et al. 2017. Host DNA released by NETosis promotes rhinovirus-induced type-2 allergic asthma exacerbation. *Nat. Med.* 23:681–691. https://doi.org/10.1038/nm.4332

Twaddell, S.H., K.J. Baines, C. Grainge, and P.G. Gibson. 2019. The Emerging Role of Neutrophil Extracellular Traps in Respiratory Disease. *Chest.* 156:774–782. https://doi.org/10.1016/j.chest.2019.06.012

Wagers, S.S., R.J. Norton, L.M. Rinaldi, J.H.T. Bates, B.E. Sobel, and C.G. Irvin. 2004. Extravascular fibrin, plasminogen activator, plasminogen activator inhibitors, and airway hyperresponsiveness. *J. Clin. Invest.* 114:104–111. https://doi.org/10.1172/JCI200419569

Wang, D., B. Hu, C. Hu, F. Zhu, X. Liu, J. Zhang, B. Wang, H. Xiang, Z. Cheng, Y. Xiong, et al. 2020. Clinical Characteristics of 138 Hospitalized Patients With 2019 Novel Coronavirus-Infected Pneumonia in Wuhan, China. *JAMA.* 323:1061–1069. https://doi.org/10.1001/jama.2020.1585

Warnatsch, A., M. Ioannou, Q. Wang, and V. Papayannopoulos. 2015. Inflammation. Neutrophil extracellular traps license macrophages for cytokine production in atherosclerosis. *Science.* 349:316–320. https://doi.org/10.1126/science.aaa8064

Wichmann, D., J.-P. Sperhake, M. Lütgehetmann, S. Steurer, C. Edler, A. Heinemann, F. Heinrich, H. Mushumba, I. Kniep, A.S. Schröder, et al. 2020. Autopsy Findings and Venous Thromboembolism in Patients With COVID-19: A Prospective Cohort Study. *Ann. Intern. Med.* 173:268–277. https://doi.org/10.7326/M20-2003

Wu, F., S. Zhao, B. Yu, Y.-M. Chen, W. Wang, Z.-G. Song, Y. Hu, Z.-W. Tao, J.-H. Tian, Y.-Y. Pei, et al. 2020. A new coronavirus associated with human respiratory disease in China. *Nature.* 579:265–269. https://doi.org/10.1038/s41586-020-2008-3

Xu, Z., L. Shi, Y. Wang, J. Zhang, L. Huang, C. Zhang, S. Liu, P. Zhao, H. Liu, L. Zhu, et al. 2020. Pathological findings of COVID-19 associated with acute respiratory distress syndrome. *Lancet Respir. Med.* 8:420–422. https://doi.org/10.1016/S2213-2600(20)30076-X

Yaqinuddin, A., and J. Kashir. 2020. Novel therapeutic targets for SARS-CoV-2-induced acute lung injury: Targeting a potential IL-1β/neutrophil extracellular traps feedback loop. *Med. Hypotheses.* 143. 109906. https://doi.org/10.1016/j.mehy.2020.109906

Yaqinuddin, A., P. Kvietys, and J. Kashir. 2020. COVID-19: Role of neutrophil extracellular traps in acute lung injury. *Respir. Investig.* 58:419–420. https://doi.org/10.1016/j.resinv.2020.06.001

Yildiz, C., N. Palaniyar, G. Otulakowski, M.A. Khan, M. Post, W.M. Kuebler, K. Tanswell, R. Belcastro, A. Masood, D. Engelberts, et al. 2015. Mechanical ventilation induces neutrophil extracellular trap formation. *Anesthesiology.* 122:864–875. https://doi.org/10.1097/ALN.0000000000000605

Zhang, X., Y. Tan, Y. Ling, G. Lu, F. Liu, Z. Yi, X. Jia, M. Wu, B. Shi, S. Xu, et al. 2020. Viral and host factors related to the clinical outcome of COVID-19. *Nature.* 583:437–440. https://doi.org/10.1038/s41586-020-2355-0

Zhou, F., T. Yu, R. Du, G. Fan, Y. Liu, Z. Liu, J. Xiang, Y. Wang, B. Song, X. Gu, et al. 2020. Clinical course and risk factors for mortality of adult inpatients with COVID-19 in Wuhan, China: a retrospective cohort study. *Lancet.* 395:1054–1062. https://doi.org/10.1016/S0140-6736(20)30566-3

Zuo, Y., S. Yalavarthi, H. Shi, K. Gockman, M. Zuo, J.A. Madison, C. Blair, A. Weber, B.J. Barnes, M. Egeblad, et al. 2020. Neutrophil extracellular traps in COVID-19. *JCI Insight.* 5. e138999. https://doi.org/10.1172/jci.insight.138999

Supplemental material

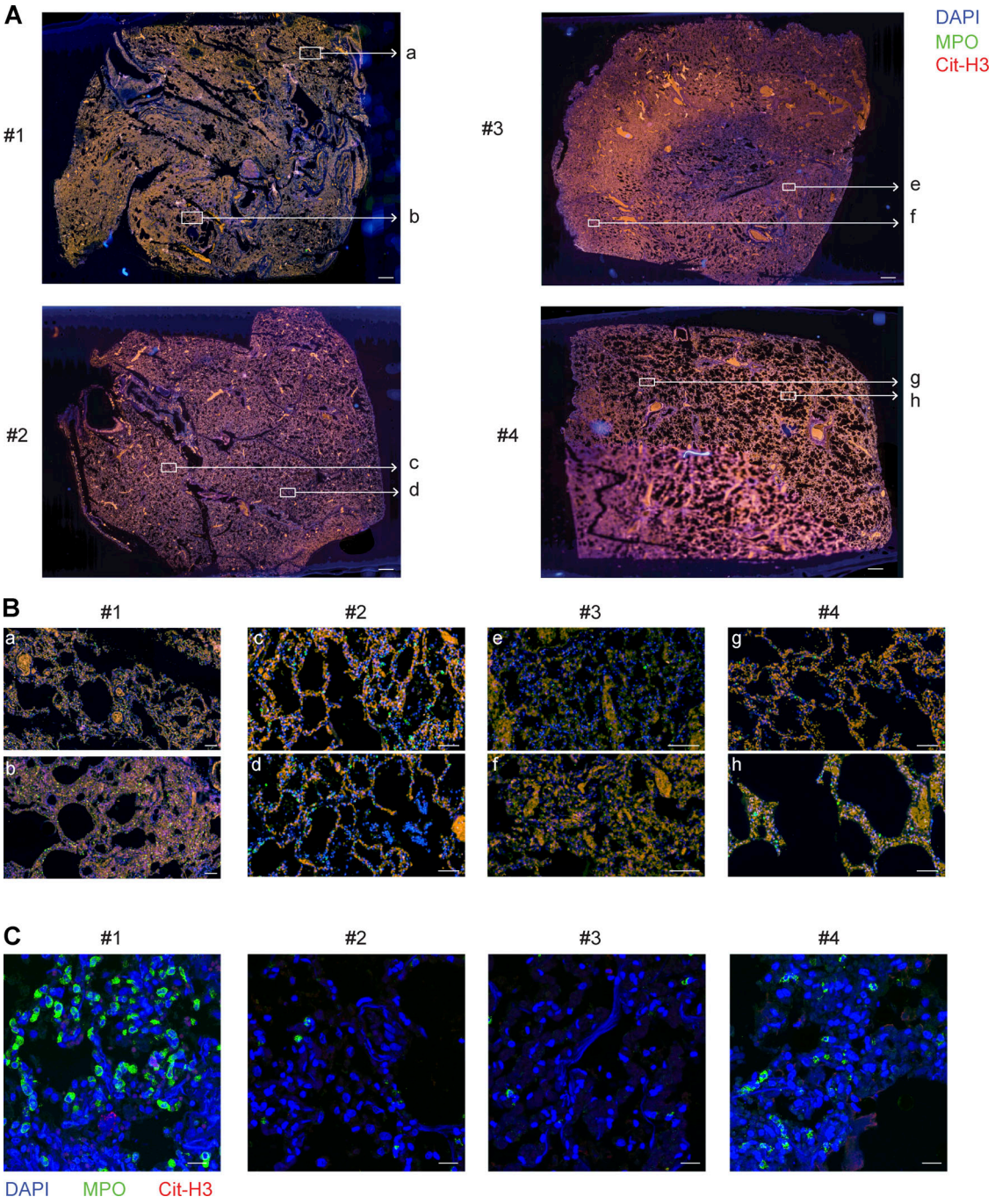

Figure S1. **No evidence of NETs in postmortem lung biopsy specimens from non–COVID-19 patients. (A)** Photographs of entire antibody-stained immunofluorescence lung sections from non–COVID-19 patients. **(B)** Magnification of NET-rich zones, indicated by white boxes in A. **(C)** Representative confocal microscopy pictures of immunofluorescence staining of lung sections from non–COVID-19 patients (MPO [red] and Cit-H3 [red] merged with DAPI [blue]). Scale bars, 1 mm (A); 100 µm (B); 20 µm (C).

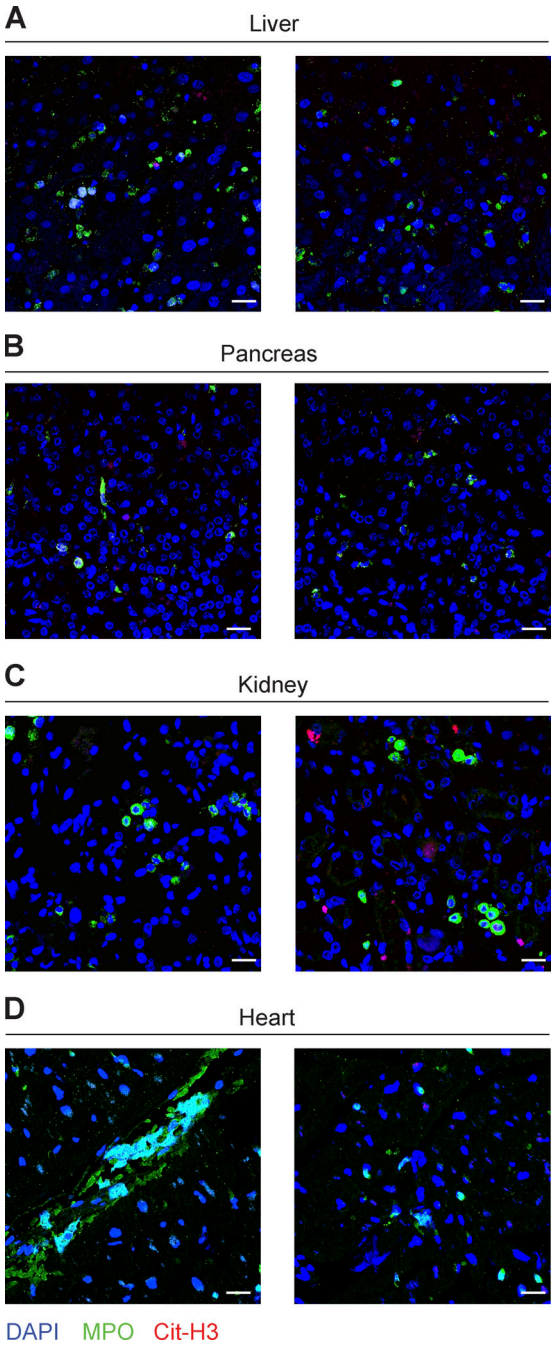

Figure S2. **No evidence of NETs in postmortem biopsy specimens from other organs in COVID-19 patients. (A–D)** Representative confocal microscopy pictures of immunofluorescence staining from (A) liver, (B) pancreas, (C) kidney, and (D) heart sections from two COVID-19 patients are shown (MPO [red] and Cit-H3 [red] merged with DAPI [blue]). Areas containing MPO^+ neutrophils are shown. Scale bars, 20 µm.

Table S1 is provided online as a separate Word file and contains demographic and clinical characteristics of the non–COVID-19 patients involved in the study.